Author's Response – Major Revision #1

In response to Dr. Benoit Montpetit:

1.1 Using weather station data to estimate TB with SMRT

- Statistical metrics for agreement between AWS and CanSWE included in Table 2
- Modified handling of ground temperature using a simple model based on AWS air temperature described in section 4.4.3, comparison with record temperatures (at other Arctic sites; Domine et al., 2018) included in Appendix A.
- Lake fractions added to Table 1 (along with vegetation characteristics)

1.2 Non-sticky sticky hard spheres – Choice of DMRT with non-sticky spheres

- Electromagnetic model switched to IBA with microwave grain size microstructure (described in Section 4.1)

1.3 Choosing the (Kelly et al., 2003) grain growth to simulate TBs

- Switched to SSA given microstructure change described above in 1.2
- SSA parameterization described in Section 4.4.4.

1.4 Using 2m air temperature to estimate depth hoar layer temperature

- Snow temperatures parameterized with linear gradient (Section 4.4.3).

1.5 Using the (Dobson et al., 1985) model to estimate the frozen ground permittivity

- Parameterized substrate following Meloche et al. (2021).

1.6 Using a static depth hoar ratio to simulate seasonally evolving tundra snowpacks1.7 Including basic atmospheric contribution at these frequencies is sensible – please do so

- Depth hoar parameterized as explicit thickness (rather than fraction)
- Depth hoar thickness left free in calibration procedure
- Comparison of dynamic depth hoar thickness, fixed thickness, and fixed fraction included in Section 4.3
- Depth Hoar Index proposed to estimate end-of-season depth hoar thickness, and expand over early season (Section 4.4.1) – similar to Lievens et al.'s (2019) Snow Index for c-band SAR

1.7 Not considering atmospheric contributions to the simulated TBs

- Simple atmospheric contributions considered following approach used in GlobSnow (i.e. Pulliainen and Grandeil, 1999)

1.8 Using a "brute-force" method to optimize the cost function

- No changes made

1.9 Validating retrieved densities with CanSWE

- Acquired stratigraphic data from Saberi et al. (2017), used to evaluate the algorithm calibrate to bulk density samples from CanSWE (Section 5.2)

In response to Dr. Michael Durand:

1. Sensitivity tests

- Sensitivity tests included to describe effect of snow density on simulated brightness temperature (considering variations in SSA, polydispersity, and layer thickness) and the effect of wind compaction (Section 4.2)
- An additional sensitivity test was drafted for the effect of layer temperature but was not included in the revised manuscript (included at the end of this document) – instead a single line was included on line 195

2. Modifications to Figure 2 (now Figure 6)

- Added units to contour lines in Figure 6a
- Added second panel (Figure 6b) showing mapping to bulk density

3. Modifications to Figure 3 (now Figure 7)

- Brightness temperature gradient included in Figure 7, along with other forcing data (snow depth, depth hoar thickness, air temperature, and simulated ground temperature)

4. Description of H Parameter

- More in depth description of H included in Section 4.3, including equations (see point 6 below)

5. Static Depth Hoar Fraction

- See 1.6 above

6. Equations for Final Density Estimates from H

- Added equations showing estimation of individual layer densities with H (Eqs. 2&3) and conversion to bulk density (Eq. 4) in Section 4.3

7. Calibration Questions

- Calibration results discussed and compared for all sites (Section 6.1)
- Example solutions at various H levels included in Figure 6

Additional Changes

- Changed radiometry data to Enhanced-Resolution Passive Microwave Daily Brightness Temperature Version 2 dataset (Brodzik et al., 2024), from 25 km L2a product
    - Allowed EASE grid cells to be closer to AWS/CanSWE site
    - Better discernment between Eureka snow course and snow survey data (Saberi et al., 2017)
    - See updated Figure 1
- Included brief description of other passive microwave snow density retrieval algorithms on line 50
- Identified potential stages of snowpack evolution to support temporal parameterization (Section 4.4)
- Included all algorithm simulations in Appendix B
- Editing for grammar/readability throughout
- Draft sensitivity test for layer temperatures (not currently included in manuscript, see point 1 above):

    Experiment 4 showed thermal emission from the wind slab is an important consideration for our model, so Experiment 5 was designed to demonstrate the effect of varying temperatures of the various media in the electromagnetic model (Fig 5). Three situations were considered where air or substrate temperature were modified by ±10 K, while the other kept constant, or where all temperatures were modified together by ±10 K. In all cases there was a linear temperature gradient in the snowpack and changes to air temperature would be reflected in snow temperature. Absolute temperature of the various media has little effect on simulated ΔTb (<1 K when varied by ±10 C), which was to be expected due to minimal permittivity differences in frozen soil (Gelinas et al., 2025). Instead, ΔTb correspond to relative temperature difference between the air and snow (~2 K between 0 to -10 C), with increasing (decreasing) ΔTb when the air is relatively colder (warmer) than the soil…

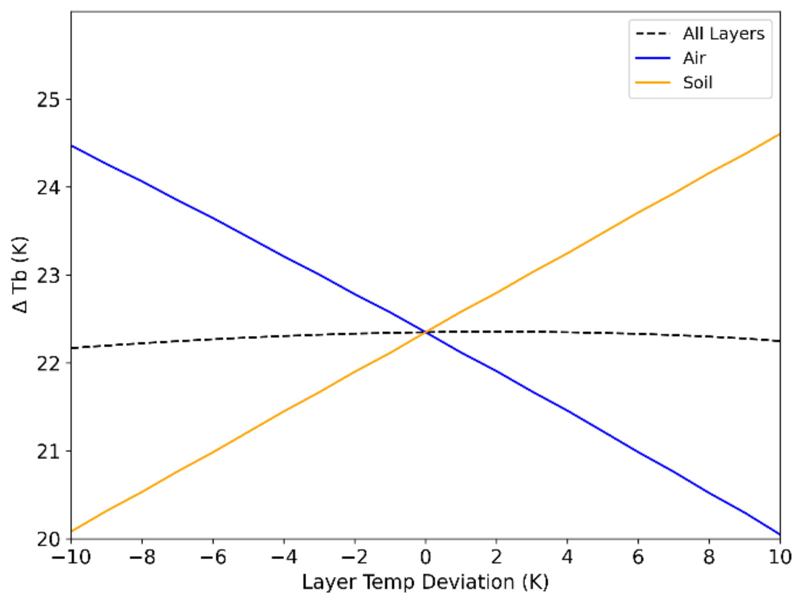

Figure 5 – Simulated microwave emission of two-layer snowpack with modified layer temperatures.

References

Brodzik, M. J., Long, D. G., and Hardman, M. A.: Calibrated Passive Microwave Daily EASE-Grid 2.0 Brightness Temperature ESDR (CETB) Algorithm Theoretical Basis Document Version 2.1, https://doi.org/10.5281/zenodo.11626219, 2024.

Domine, F., Belke-Brea, M., Sarrazin, D., Arnaud, L., Barrere, M., and Poirier, M.: Soil moisture, wind speed and depth hoar formation in the Arctic snowpack, Journal of Glaciology, 64, 990–1002, https://doi.org/10.1017/jog.2018.89, 2018.

Gelinas, A., Filali, B., Langlois, A., Kelly, R., Mavrovic, A., Demontoux, F., & Roy, A.: New wideband large aperture open-ended coaxial microwave probe for soil dielectric characterization. IEEE Transactions on Geoscience and Remote Sensing, 63, https://doi.org/10.1109/TGRS.2025.3539532, 2025.

Kelly, R., Chang, A. T., Tsang, L., and Foster, J. L.: A prototype AMSR-E global snow area and snow depth algorithm, IEEE Transactions on Geoscience and Remote Sensing, 41, 230–242, https://doi.org/10.1109/TGRS.2003.809118, 2003.

Lievens, H., Demuzere, M., Marshall, H. P., Reichle, R. H., Brucker, L., Brangers, I., de Rosnay, P., Dumont, M., Girotto, M., Immerzeel, W. W., Jonas, T., Kim, E. J., Koch, I., Marty, C., Saloranta, T., Schöber, J., and De Lannoy, G. J. M.: Snow depth variability in the Northern Hemisphere mountains observed from space, Nat Commun, 10, https://doi.org/10.1038/s41467-019-12566-y, 2019.

Meloche, J., Royer, A., Langlois, A., Rutter, N., and Sasseville, V.: Improvement of microwave emissivity parameterization of frozen Arctic soils using roughness measurements derived from photogrammetry, Int J Digit Earth, 14, 1380–1396, https://doi.org/10.1080/17538947.2020.1836049, 2021.

Pulliainen, J. and Grandeil, J.: HUT snow emission model and its applicability to snow water equivalent retrieval, IEEE Transactions on Geoscience and Remote Sensing, 37, 1378–1390, https://doi.org/10.1109/36.763302, 1999.

Saberi, N., Kelly, R., Toose, P., Roy, A., and Derksen, C.: Modeling the observed microwave emission from shallow multi-layer Tundra Snow using DMRT-ML, Remote Sens (Basel), 9, https://doi.org/10.3390/rs9121327, 2017.